Development of tungsten fiber reinforced tungsten with porous matrix

Y.Mao[a], J.W.Coenen[a], S.Sistla[c], X.Tan[d], J.Riesch[b], L.Raumann[a], D. Schwalenberg[a], T. Höschen[b], C.Chen[d], Y.Wu[d], C.Broeckmann[c] and Ch.Linsmeier[a]

[a] Forschungszentrum Jülich GmbH, Institut für Energie- und Klimaforschung - Plasmaphysik, Partner in the Trilateral Euregio Cluster, 52425 Jülich, Germany

[b] Max-Planck-Institut für Plasmaphysik, 85748 Garching b. München, Germany

[c] Institut für Werkstoffanwendungen im Maschinenbau (IWM), RWTH Aachen University, 52062 Aachen, Germany

[d]School of Materials Science and Engineering, Hefei University of Technology, 230009 Hefei, China

Abstract

In future fusion reactors, tungsten is a main candidate material for the plasma facing material. To overcome the brittleness of tungsten, tungsten fiber-reinforced tungsten (W_f/W) composites have been developed using a powder metallurgy processes. In this study, a novel type of W_f/W with porous matrix has been developed using field assisted sintering technology (FAST). Compared to conventional W_f/W, the avoiding of fiber/matrix interface simplified the production process. Initial mechanical testing showed W_f/W with porous matrix can establish a promising pseudo ductile behavior with an increased fracture toughness compared to pure W.

Introduction

The extreme environment of the first wall of a fusion reactor puts unique challenges on materials and requires advanced mechanical and thermal properties. Tungsten (W) is the main candidate material for the plasma facing material in fusion reactor [1, 2], as it is resilient against erosion, has the highest melting point of all metals and shows rather benign behavior under neutron irradiation [3]. However, the intrinsic brittleness of tungsten could cause some potential issue in the future fusion environment with high transient heat loads and neutron irradiation. To overcome this drawback, tungsten fiber reinforced tungsten (W_f/W) composites has been intensively developed relying on an extrinsic toughening principle [4-8]. In recent studies, a process using field assisted sintering technology (FAST) to produce W_f/W has been established [9-11]. FAST is a low voltage, pulsed direct current (DC) activated, pressure-assisted sintering, and synthesis technique. During the process, the fiber/powder mixture is consolidated to a bulk material relying on current Joule heating under a uniaxial pressure in the mold. In cooperation with a weak oxide interface and high strength tungsten fibers, a pseudo ductile fracture behavior can be achieved as demonstrated in previous studies [9, 12]. It has been reported that, a relatively weak interface between the fiber and the matrix is beneficial to realize the pseudo-ductility of the composites [12-14]. The improved fracture resistance relies on the extra energy dissipation mechanisms like interface debonding, crack bridging by the fibers and fiber pull-out.

However, due to the inclusion of an oxide interface, some problems are potentially being introduced, e.g, interface delamination on the surface under high heat flux exposure [15]. What is more important is that, currently, the interface production is very costly in terms of time and money due to the use of magnetron sputtering [12]. It is the bottle neck in the production process of W_f/W. Other coating techniques are under investigation and not yet feasible for short fibers. Therefore, it

would bring a great benefit in terms of large scale production, if the application of interface can be avoided. Porous matrix composites offer a possible solution as an alternative to the conventional weak interface composites.

Tungsten fiber reinforced tungsten with porous matrix

For fiber reinforced composites with brittle matrix, damage tolerance is obtained when the matrix acts as a mechanical "buffer" between adjacent fibers, so that the cracks from the matrix should not penetrate into the fibers. Fiber breakage should remain isolated with minimal stress concentration in neighboring fibers. It can be seen from previous W_f/W studies [12] that, if no interphase is applied between fiber and matrix, the crack can easily penetrate through the fibers, and thus, the fracture resistance cannot be enhanced.

The buffer zone between fiber and matrix can be enabled in two ways. Conventionally, fiber coating is used to promote crack deflection, fiber/matrix debonding and frictional sliding along the fiber/matrix interfaces (Figure 1a). This principle is used in the previous development of W_f/W [7, 12, 16]. Another approach involves the use of a controlled amount of fine-scale matrix porosity, obviating the need for a fiber coating (Figure 1b). This approach can be viewed as an extension of the weak coating concept. For this case, the crack deflection occurs because of the low strength of the porous interphase and its poor cohesion with the fibers [17, 18]. This principle has also been widely used like in carbon fiber reinforced carbon (CFC) or silicon carbide fiber reinforced silicon carbide (SiC/SiC) [19].

In this study, the porous matrix composites principle is used in the design of W_f/W. A porous matrix is realized by reducing the sintering temperature during the FAST process. Another potential advantage of decreasing the process temperature is that the fiber recrystallization and

grain growth during the sintering is mitigated. This is helpful to retain good fiber mechanical properties [20, 21].

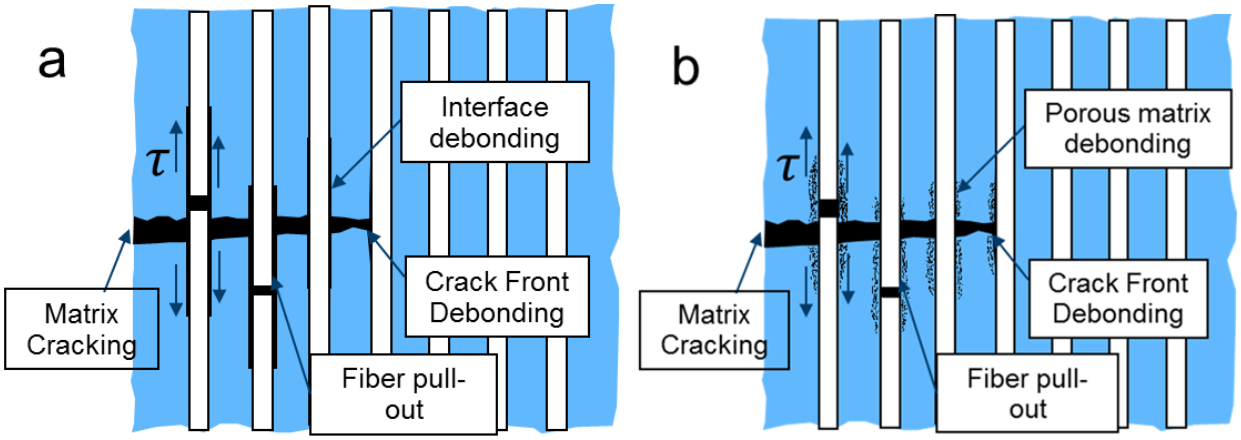

Figure 1 Schematics of the damage processes that enable damage tolerance in a) conventional dense-matrix fiber reinforced composites with weak-interface and b) porous matrix fiber reinforced composites without fiber coatings [17].

Production process

Similar to conventional W_f/W production, the raw materials of the porous matrix W_f/W fabrication are pure tungsten powders (provided by OSRAM GmbH) with 5 µm average particle size (fischer sub sieve size) and potassium doped short tungsten fibers (provided by OSRAM GmbH) with 2.4 mm length and 0.15 mm diameter. The tungsten fibers were produced by a drawing process and then cut into the required length. Due to the drawn microstructure with elongated grains, the tungsten fibers have extremely high tensile strength (~3000 MPa) with ductile fracture behavior at room temperature [21, 22]. Potassium doping is aiming for an advanced high temperature microstructural stability, since potassium (approx. 75 ppm) is present in form of nano-dispersed bubble rows along the elongated grains pinning the grain boundaries [21, 23].

Table 1 FAST process parameters for conventional W_f/W and porous matrix W_f/W [12].

Sintering parameters	**Conventional W_f/W**	**Porous matrix W_f/W**
Temperature	1900 °C	1550 °C
Pressure	60 MPa	60 MPa
Time	4 min	4 min
Heating rate	100 °C/min	100 °C/min
Relative density	~93%	~88%
Fiber volume fraction	30%	40%
Fiber/matrix interlayer	With yttria interface	no

During the production, the tungsten fibers were mixed with the tungsten powders by manual shaking in a vessel in order to get the random distribution of the tungsten fibers. The fiber weight fraction in the mixture was 40%. About the fiber volume fraction, for conventional W_f/W, yttrium oxide is used as the interface between fiber and matrix. In this case, with the increasing fiber volume fraction, the content of the weak yttrium oxide interface will also be higher. If the content of the weak layer in the composites is too high, the strength of the material will decrease due to the early failure of the weak yttrium oxide [12]. Therefore, 30% fiber volume fraction is an optimized value balancing material strength and fracture behavior (This results will be publish in a later study). For porous matrix W_f/W, since no weak layer is involved, higher fiber volume fraction can be applied. For other porous matrix composites, like SiC/SiC or CFC, fiber volume fraction is normally higher than 50% [17]. Therefore, as the first attempt, 40% of fiber volume fraction is used for the porous matrix W_f/W.

The production parameters of the FAST process is shown in Table 1, with the comparison to typical parameters used in conventional-W_f/W process [12]. During the FAST process, the powder/fiber mixture is consolidated in a graphite die with 40 mm inner diameter. W foil was used to separate the sample and the graphite mold in order to reduce the carbon contamination [10, 24]. Based on the results in [24], if a W foil is not added to separate the mold and the sample, C contamination will be detected in the W fibers after FAST process. Nanosized carbides in the grains and the carbide-layer on the grain boundaries are formed during the production. This C contamination will cause embrittlement of W fibers. Therefore, for recent research, all the W_f/W production by FAST, W foil-protection is used. The sintering was performed under vacuum below 0.1 mbar. As result, a coin shape sample (40 mm diameter and ~5 mm height) was produced. The relative density of the samples after sintering is around 88 % according to the density measurement using the Archimedes principle.

Mechanical characterization and thermal diffusivity measurement

To study the fracture behavior of the porous matrix composites, an in-situ 3-point bending test is performed similar to the test in [25]. The samples are manufactured based on the EU standards DIN EN ISO 148-1 and 14556: 2006–10 [26]. The sample dimensions (KLST geometry) are [27]: 3 mm x 4mm x 27 mm, 22 mm span, 1 mm V-notch depth, 0.1 mm notch root radius, shaped by Electrical discharge machining (EDM) without further surface and notch modification.

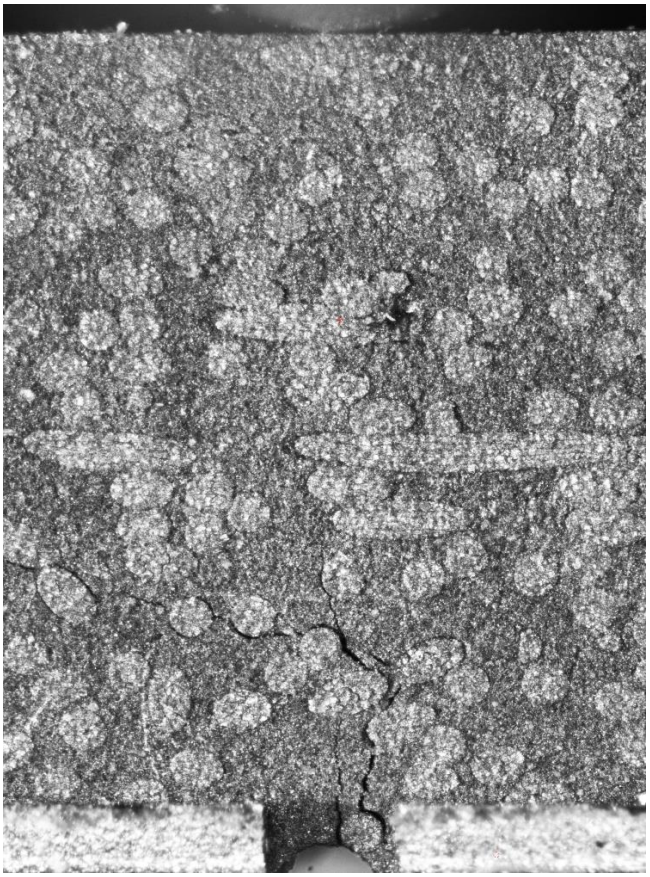

Figure 2 image from the tracking camera during the bending test showing the crack length.

A universal testing device (TIRAtest 2820, Nr. R050/01, TIRA GmbH) with an optical camera system (DU657M Toshiba) is used to perform the test. The displacement speed is 1 µm/s is used The camera system is to track crack behavior and measure the absolute sample movement. One typical tracking image during the experiment is shown in Figure 2. As result, a force-displacement curve can be then determined. The vertical movement of the sample relative to the reference stage is defined as the sample displacement. Two samples are tested and compared to the conventional W_f/W in a previous study [28].

Apart from the force-displacement curve, fracture toughness (K_q) are also be calculated based on ASTM E399 standard:

$$K_q = \frac{P \cdot S}{B \cdot W^{3/2}} \cdot f(a_f/W) \quad (1)$$

Where P is the maximum load during stable crack growing, S is the distance between the support pins, B is the sample width, W is the sample thickness, a_f is the stable crack length which equals to the pre-notch length plus the crack extension length, the function $f(a_f/W)$ is described in ASTM E399 as:

$$f\left(\frac{a_f}{W}\right) = \frac{3\left(\frac{a_f}{W}\right)^{\frac{1}{2}}\left\{1.99-\left(\frac{a_f}{W}\right)\left(1-\frac{a_f}{W}\right)\left(2.15-\frac{3.93a_f}{W}+\frac{2.7{a_f}^2}{W^2}\right)\right\}}{2\left(1+\frac{2a_f}{W}\right)\left(1-\frac{a_f}{W}\right)^{\frac{3}{2}}} \quad (2)$$

In this study, the \crack extension length (a_f) is measured by the in-situ tracking image as the surface crack length. The corresponding force before the unstable load drop is used as the maximum loading.

To investigate the high porosity influence on the thermal conductivity properties, a thermal diffusivity measurement is performed from room temperature to 450 °C by using a laser flash diffusivity system (LFA457, Germany). The specimen dimension is a disc with 6 mm in diameter and 2 mm in thickness. The testing atmosphere is Ar. For comparison, the thermal diffusivity of a conventional W_f/W sample [25] with ~94% density, 30% fiber volume fraction and 1.5 μm yttrium oxide fiber/matrix interface is also measured.

Results and discussions

The force-displacement curves of the porous matrix W_f/W during the 3-point bending test are shown in Figure 3. Typical force-displacement curves of the conventional W_f/W and pure W from previous study are also included for comparison [28].

From Figure 3, it can be seen that, a pseudo ductile behavior can be established by both porous matrix W_f/W samples [12]: after an linear-elastic deformation, the slope of the curve changes gradually to zero with several small load drops; then a massive load-drop happens after reaching the maximum force; afterwards, the samples tend to have a stepwise or continuous load-decreasing. After the 3-point bending test, typical sample overview is shown in Figure 4. Even after large deformation (vertical bending displacement >0.3 mm), the sample remains whole with a strength of over 50 N.

Compared to conventional W_f/W in Figure *3* and typical samples in [28], the maximum loading is lower, but the deformation ability before massive load-drop is larger. During the elastic deformation stage, the slope of the porous matrix W_f/W is lower compared to conventional W_f/W and pure W. This effect can be attributed to the lower density.

Another noticeable point is that, the strength/maximum loading of the porous matrix W_f/W is lower compared to the conventional W_f/W due to the much weaker matrix. This is compromise that has to be made when using the porous matrix composites. Because in the absence of fiber coatings, the matrix must be sufficiently weak to enable damage tolerance under fiber-dominated loadings. This weak matrix will reduce the strength properties of the material. But the decrease of the strength could potentially be compensated by increasing the fiber volume fraction, which will be discussed in future work.

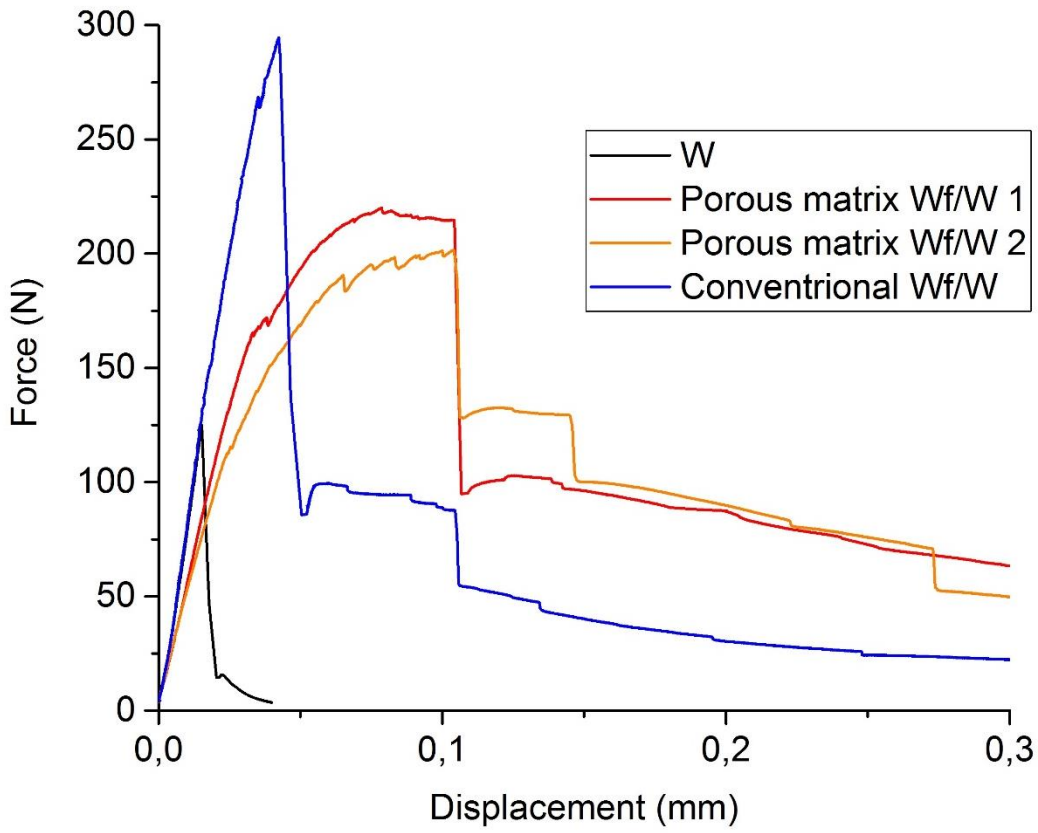

Figure 3 force displacement curves of porous matrix W_f/W compared to typical conventional W_f/W and pure W

Figure 4 typical porous matrix W_f/W after the 3-point bending test

To analyze the fracture surface, the sample in Figure 4 is broken apart manually after the bending test. The SEM analysis on the fracture surface is shown in Figure 5. The uneven topology of the surface is an indication for crack deflection. Additionally, fiber/matrix interface debonding is

observed. Notable fiber pull-out effect can be also observed. Some clear fiber end edges without fracture are also visible, indicating the fiber-ends pull-out from the matrix.

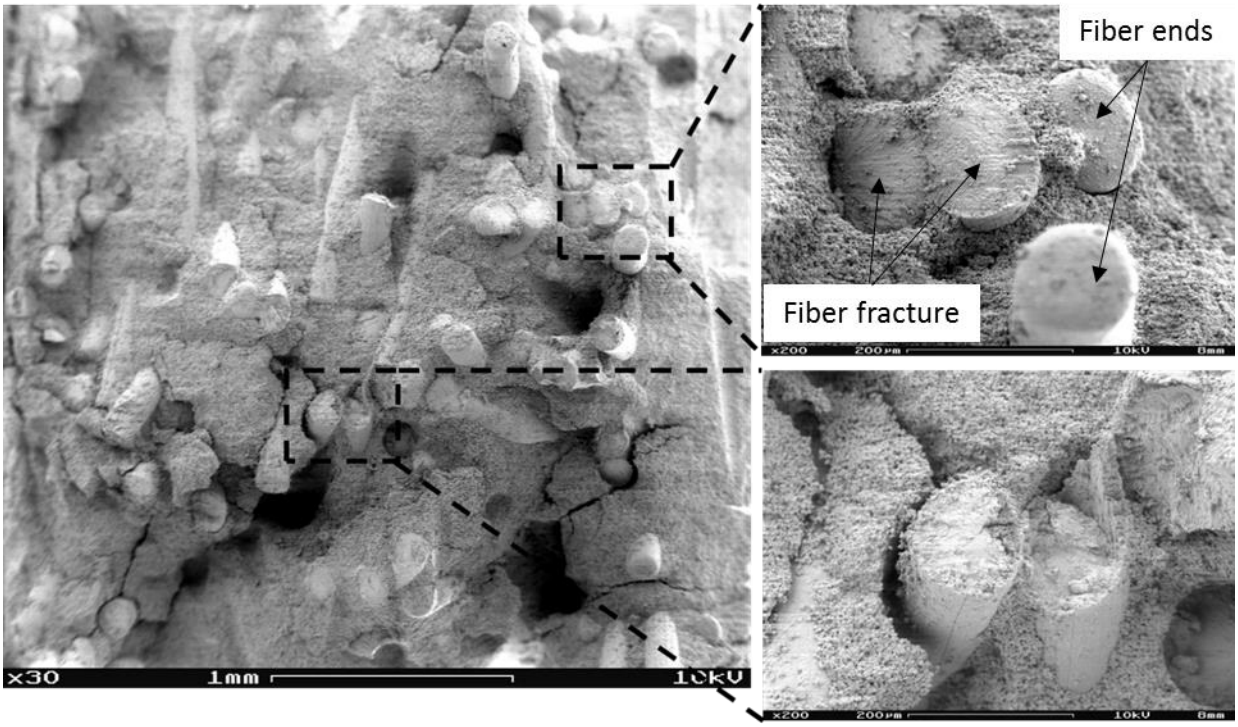

Figure 5 fracture surface after 3-point bending test

Based on the quantitatively measured force-displacement curves, and the tracking image during the test, fracture toughness (K_q) are calculated based on equation (1) similar to a previous study [28]. The results are shown in Table 2, together with the fracture toughness of conventional W_f/W and pure W produced by FAST from a previous study [28]. It is necessary to state that all the average fracture toughness listed here are only based on limited number of tests. Also, the sample dimension is smaller compared to the standard test. Therefore, large scattering of the results can be expected. However, from Table 2, it is still safe to conclude that the fracture toughness of porous matrix W_f/W is much higher than pure W and comparable to conventional W_f/W. Compared to the

previous study on fracture toughness of polycrystalline W material [29], the porous matrix W_f/W can give comparable value with the rolled and drawn W material.

Table 2 fracture toughness of porous matrix W_f/W, compared to the previous study on fracture toughness of W_f/W and polycrystalline W material [29]

Samples	Fracture toughness K_q (MPa $m^{0.5}$)
Pure tungsten	5±1
Conventional W_f/W	28±9
Porous matrix W_f/W	30±1
Polycrystalline W (as sintered) [29]	5.1
Polycrystalline W (Rolled and drawn) [29]	35.1

Based on the results above, it can be concluded that the porous matrix W_f/W shows a promising pseudo ductile behavior with an increased damage tolerance compared to pure W. Similar to conventional W_f/W, fiber bridging, fiber pull-out, crack deflection and interface debonding are likely the energy dissipation mechanisms contributing to the elevated fracture resistance.

The thermal diffusivity of porous matrix W_f/W is shown in Figure 6, compared to conventional W_f/W and reference pure W [30]. It can be seen from the results, both conventional W_f/W and porous matrix W_f/W show lower thermal diffusivity compared to reference W, due to the higher porosity. The thermal diffusivity of porous matrix is ~82% of the value for pure W. This decreasing of the thermal conductivity property will indeed have some influence on the heat exhaust when using as plasma facing materials. However, since the thermal conductivity of tungsten is already quite high, this decreased thermal conductivity is still acceptable when considering the increased mechanical properties. Additionally, for the next step, the fiber volume fraction of porous matrix

W_f/W will be optimized. When higher fiber volume fraction is applied, the density of the porous matrix W_f/W will further be increased which will promote the thermal conductivity behavior of porous matrix W_f/W.

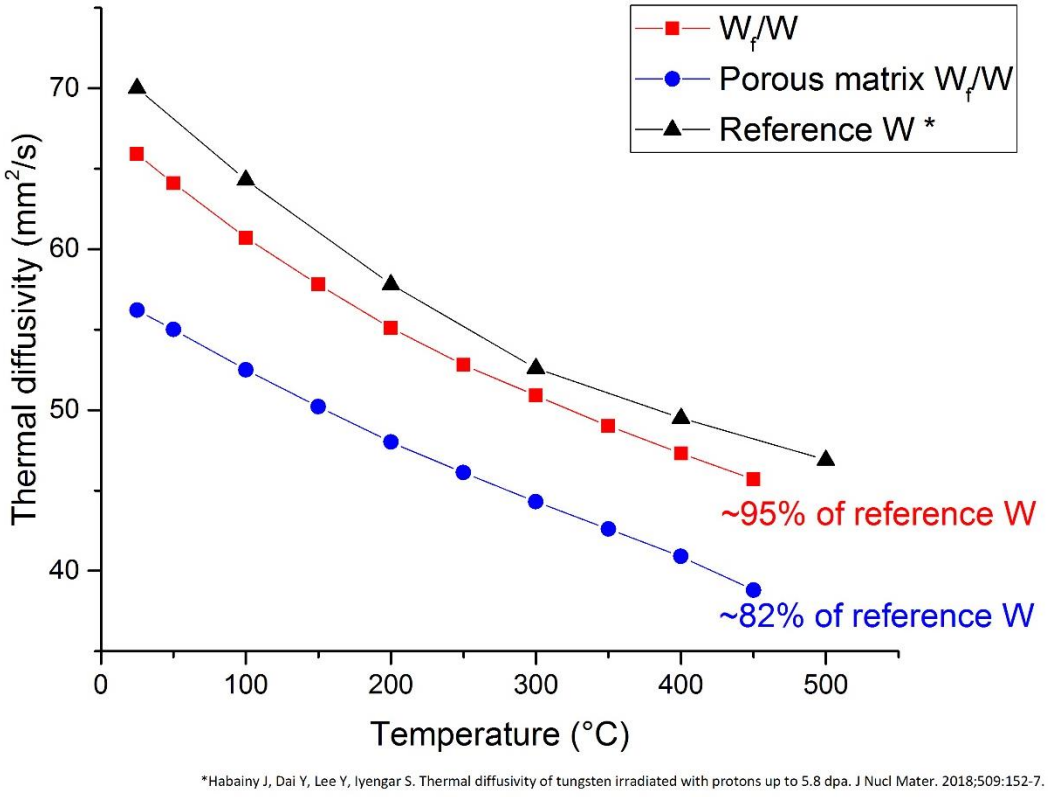

Figure 6 thermal diffusivity of porous matrix W_f/W compared to conventional Wf/W and reference pure W [30].

Summary and outlook

In this work, porous matrix W_f/W is produced by field assisted sintering technology for the first time. 3-point bending tests are performed to understand the fracture behavior of the material. The results are compared to pure tungsten produced by FAST and conventional W_f/W. Based on the initial results, porous matrix W_f/W can achieve a promising defect tolerance. Compared to

conventional W_f/W, the production process is much easier due to the omission of the interface coating, which is a great benefit considering the large scale production in near future.

For the next step, the porous matrix needs to be further optimized aiming for better material properties. Fiber volume fraction and sample density are the most critical points that need to be adjusted. Investigations are already being carried out in terms of these aspects and will be discussed in a future publication.

Apart from further optimization of the material properties, when using porous matrix W_f/W in the plasma facing component, other properties need to be considered, like hydrogen retention and oxidation behavior in case of an accidental air inrush. For hydrogen retention, based on the study in [6], the pores in W_f/W are mainly open pores. Therefore, a dramatically increase of the hydrogen retention is not expected. The oxidation behavior of porous matrix W_f/W could be potentially improved by combining the idea of self-passivating W alloy [31]. These points will be investigated in following studies.

Acknowledgements

This work has been carried out within the framework of the EUROfusion Consortium and has received funding from the Euratom research and training programme 2014-2018 and 2019-2020 under grant agreement No 633053. The views and opinions expressed herein do not necessarily reflect those of the European Commission.

Reference

[1] Philipps V. Tungsten as material for plasma-facing components in fusion devices. J Nucl Mater. 2011;415(1):S2-S9.

[2] Coenen JW, Antusch S, Aumann M, Biel W, Du J, Engels J, et al. Materials for DEMO and reactor applications—boundary conditions and new concepts. Physica Scripta. 2016;2016(T167):014002.

[3] Smid I, Akiba M, Vieider G, Plöchl L. Development of tungsten armor and bonding to copper for plasma-interactive components. J Nucl Mater. 1998;258-263(Part 1):160-72.

[4] Riesch J, Buffiere JY, Höschen T, di Michiel M, Scheel M, Linsmeier C, et al. In situ synchrotron tomography estimation of toughening effect by semi-ductile fibre reinforcement in a tungsten-fibre-reinforced tungsten composite system. Acta Materialia. 2013;61(19):7060-71.

[5] Gietl H, von Muller A, Coenen JW, Decius M, Ewert D, Hoschen T, et al. Textile preforms for tungsten fibre-reinforced composites. Journal Of Composite Materials. 2018;52(28):3875-84.

[6] Mao Y, Coenen JW, Riesch J, Sistla S, Chen C, Wu Y, et al. Spark Plasma Sintering Produced W-Fiber-Reinforced Tungsten Composites. In: Cavaliere P, editor. Spark Plasma Sintering of Materials: Advances in Processing and Applications. Cham: Springer International Publishing; 2019. p. 239-61.

[7] Gietl H, Riesch J, Coenen JW, Hoschen T, Linsmeier C, Neu R. Tensile deformation behavior of tungsten fibre-reinforced tungsten composite specimens in as-fabricated state. Fusion Engineering And Design. 2017;124:396-400.

[8] Du J, Höschen T, Rasinski M, Wurster S, Grosinger W, You JH. Feasibility study of a tungsten wire-reinforced tungsten matrix composite with ZrOx interfacial coatings. Composites Science and Technology. 2010;70(10):1482-9.

[9] Mao Y, Coenen JW, Riesch J, Sistla S, Almanstötter J, Jasper B, et al. Development and characterization of powder metallurgically produced discontinuous tungsten fiber reinforced tungsten composites. Physica Scripta. 2017;T170:014005.

[10] Coenen JW, Mao Y, Sistla S, Riesch J, Hoeschen T, Broeckmann C, et al. Improved pseudo-ductile behavior of powder metallurgical tungsten short fiber-reinforced tungsten (Wf / W). Nuclear Materials and Energy. 2018;15:214-9.

[11] Coenen JW, Mao Y, Almanstotter J, Calvo A, Sistla S, Gietl H, et al. Advanced materials for a damage resilient divertor concept for DEMO: Powder-metallurgical tungsten-fibre reinforced tungsten. Fusion Engineering And Design. 2017;124:964-8.

[12] Mao Y, Coenen JW, Riesch J, Sistla S, Almanstotter J, Jasper B, et al. Influence of the interface strength on the mechanical properties of discontinuous tungsten fiber-reinforced tungsten composites produced by field assisted sintering technology. Compos Part a-Appl S. 2018;107:342-53.

[13] Czél G, Wisnom MR. Demonstration of pseudo-ductility in high performance glass/epoxy composites by hybridisation with thin-ply carbon prepreg. Composites Part A: Applied Science and Manufacturing. 2013;52:23-30.

[14] Ming-Yuan H, Hutchinson JW. Crack deflection at an interface between dissimilar elastic materials. International Journal of Solids and Structures. 1989;25(9):1053-67.

[15] Coenen JW, Mao Y, Sistla S, Müller Av, Pintsuk G, Wirtz M, et al. Materials development for new high heat-flux component mock-ups for DEMO. Fusion Engineering and Design. 2019.

[16] Du J, You J-H, Höschen T. Thermal stability of the engineered interfaces in Wf/W composites. Journal of Materials Science. 2012;47(11):4706-15.

[17] Zok FW, Levi CG. Mechanical Properties of Porous-Matrix Ceramic Composites. Advanced Engineering Materials. 2001;3(1-2):15-23.

[18] Mackin TJ, Yang JY, Levi CG, Evans AG. Environmentally compatible double coating concepts for sapphire fiber-reinforced γ-TiAl. Materials Science and Engineering: A. 1993;161(2):285-93.

[19] Brennan JJ. Interfacial characterization of a slurry-cast melt-infiltrated SiC/SiC ceramic-matrix composite. Acta Materialia. 2000;48(18):4619-28.

[20] Riesch J, Almanstötter J, Coenen JW, Fuhr M, Gietl H, Han Y, et al. Properties of drawn W wire used as high performance fibre in tungsten fibre-reinforced tungsten composite. IOP Conference Series: Materials Science and Engineering. 2016;139:012043.

[21] Riesch J, Han Y, Almanstotter J, Coenen JW, Hoschen T, Jasper B, et al. Development of tungsten fibre-reinforced tungsten composites towards their use in DEMO-potassium doped tungsten wire. Physica Scripta. 2016;T167(T167):014006.

[22] Zhao P, Riesch J, Hoschen T, Almanstotter J, Balden M, Coenen JW, et al. Microstructure, mechanical behaviour and fracture of pure tungsten wire after different heat treatments. Int J Refract Met H. 2017;68:29-40.

[23] Linsmeier C, Rieth M, Aktaa J, Chikada T, Hoffmann A, Hoffmann J, et al. Development of advanced high heat flux and plasma-facing materials. Nucl Fusion. 2017;57(9):092007.

[24] Mao Y, Chen C, Coenen JW, Riesch J, Sistla S, Almanstötter J, et al. On the nature of carbon embrittlement of tungsten fibers during powder metallurgical processes. Fusion Engineering and Design. 2019;145:18-22.

[25] Mao Y, Coenen JW, Riesch J, Sistla S, Almanstötter J, Reiser J, et al. Fracture behavior of random distributed short tungsten fiber-reinforced tungsten composites. Nucl Fusion. 2019;59(8):086034.

[26] Rieth M, Hoffmann A. Influence of microstructure and notch fabrication on impact bending properties of tungsten materials. International Journal of Refractory Metals and Hard Materials. 2010;28(6):679-86.

[27] Prüfung metallischer Werkstoffe; Kerbschlagbiegeversuch; Besondere Probenform und Auswertungsverfahren. s.l. DIN 50115: Beuth-Verlag; 1991.

[28] Mao Y, Coenen JW, Riesch J, Sistla S, Almanstötter J, Reiser J, et al. Fracture behavior of random distributed short tungsten fiber-reinforced tungsten composites Nucl Fusion. 2019;accepted.

[29] Gludovatz B, Wurster S, Hoffmann A, Pippan R. Fracture toughness of polycrystalline tungsten alloys. International Journal of Refractory Metals and Hard Materials. 2010;28(6):674-8.

[30] Habainy J, Dai Y, Lee Y, Iyengar S. Thermal diffusivity of tungsten irradiated with protons up to 5.8 dpa. J Nucl Mater. 2018;509:152-7.

[31] Litnovsky A, Wegener T, Klein F, Linsmeier C, Rasinski M, Kreter A, et al. Smart alloys for a future fusion power plant: First studies under stationary plasma load and in accidental conditions. Nuclear Materials and Energy. 2017;12:1363-7.